Research Article

Ganeshkumar Selvaraj, Sureshbabu Yessian, Sureshkumar Ramalingam, Selvan Dharani Kumar, Gokilakrishnan Gopal, Shubham Sharma*, Abhinav Kumar, Changhe Li, and Mohamed Abbas*

Investigation on topology-optimized compressor piston by metal additive manufacturing technique: Analytical and numeric computational modeling using finite element analysis in ANSYS

https://doi.org/10.1515/phys-2022-0259
received November 14, 2022; accepted June 07, 2023

Abstract: Air compressors are widely used in factories to power automation systems and store energy. Several studies have been conducted on the performance of reciprocating and screw compressors. Advancements in design and manufacturing techniques, such as generative design and topology optimization, are leading to improved performance and turbomachinery growth. This work presents a methodology to design and manufacture air compressor pistons using topology optimization and metal additive manufacturing. The existing piston is converted to 3D CAD data and topology optimization is conducted to reduce material in stress concentration regions. Thermal and mechanical loads are considered in boundary conditions. The results show reduced material and improved efficiency, which is validated using ANSYS fluent. The optimized 3D model of the piston is too complex for conventional subtractive manufacturing, so laser sintering 3D printing is proposed. Honeycomb pattern infill patterns are used in 3D printing. This investigation is a step toward researching similar methods in other reciprocating compressor components such as cylinder, cylinder head, piston pins, crankshaft, and connecting rods, which will ultimately lead to improved compressor efficiency.

Keywords: compressor piston, topology optimization, metal 3D printing, additive manufacturing, LASER sintering, fusion 360, ANSYS fluent

*** Corresponding author: Shubham Sharma,** Mechanical Engineering Department, University Centre for Research and Development, Chandigarh University, Mohali, 140413, Punjab, India; School of Mechanical and Automotive Engineering, Qingdao University of Technology, 266520, Qingdao, China; Department of Mechanical Engineering, Lebanese American University, Kraytem 1102-2801, Beirut, Lebanon, e-mail: shubhamsharmacsirclri@gmail.com, shubham543sharma@gmail.com

*** Corresponding author: Mohamed Abbas,** Electrical Engineering Department, College of Engineering, King Khalid University, Abha 61421, Saudi Arabia, e-mail: mabas@kku.edu.sa

Ganeshkumar Selvaraj, Sureshbabu Yessian, Sureshkumar Ramalingam, Gokilakrishnan Gopal: Department of Mechanical Engineering, Sri Eshwar College of Engineering, Coimbatore 641202, Tamil Nadu, India

Selvan Dharani Kumar: Department of Mechanical Engineering, KPR Institute of Engineering and Technology, Coimbatore 641707, Tamil Nadu, India

Abhinav Kumar: Department of Nuclear and Renewable Energy, Ural Federal University Named After the First President of Russia, Boris Yeltsin, 19 Mira Street, 620002, Ekaterinburg, Russia, e-mail: drabhinav@ieee.org

Changhe Li: School of Mechanical and Automotive Engineering, Qingdao University of Technology, 266520, Qingdao, China

1 Introduction

Material selection and design optimization play a vital role in all finished products. The optimization involves weight reduction and an increase in the performance of the machines. In industry 4.0, automation industries utilize pneumatic devices such as cylinders, direction control valves, regulators, *etc.* [1,2]. The primary source of the pneumatic system is air compressors. The increasing weight of the moving parts leads to a rise in power consumption. Several types of research have been carried out on power reduction by weight optimization and changing the metallurgy of machine components [3–5]. Topology optimization is the mathematical method to optimize the distribution of materials based on the mechanical and thermal stresses acting on the material. Software like ANSYS, Abaqus, TOSCA, and Solid works is equipped with topology optimization [6,7]. Topology optimization is an algorithmic technique that yields the most efficient design of the components. The method works by removal of material based on boundary conditions and

Open Access. © 2023 the author(s), published by De Gruyter. This work is licensed under the Creative Commons Attribution 4.0 International License.

constraints given the object [8–10]. The finite element method and finite volume computation techniques are equipped with the topology optimization algorithm for the reduction of materials to yield the most efficient designs [11]. In refrigerators, a vapor compression system is achieved using compressors. The component's temperature increases in the compression cycle, and the temperature reduction happens in expansion [12,13]. There are various compressor piston parts such as spring plates, wafer plates, ported plates, valve plates, lock nuts, studs, gudgeon pins, and radius rings [14–16]. The piston is considered a significant component needed to optimize the structure. Carbon peeks, peek, and nylon thermoplastic materials are used to manufacture piston accessories such as rings and plates [17–19].

The piston is the main component of reciprocating air compressors and internal combustion engines [20]. This main reciprocating mass is subjected to inertial and compressive forces [21,22]. The piston needs to withstand high temperature, and high pressure for turbochargers. Advanced spark ignition engines need high compression ratios, for which component design and optimization are essential to reduce the size of the machine [23–25]. Power consumption is an additional factor that attracts the user to the optimized brands of compressors. In this scenario, aluminum is not only the best choice but steel alloys for increasing performance and fulfilling high thermal and mechanical loads [26]. The kinematic behavior of the piston assembly and cranking behavior under different loads need to be considered. Several types of research have been carried out in material optimization and design topology optimization of piston components [27]. Based on the load distribution, the reduction of material under topology optimization should balance the weight ratio. The higher density materials lead to increase the weight of component [28]. In the conventional subtractive manufacturing process, the complexity of the component needs to be considered while in the design stage. The modern industry 4.0 scenario unveils modern ways of manufacturing through additive manufacturing [29]. The design obtained after the topology optimization can be easily manufactured layer by layer. This is a promising technology for manufacturing complex shape components with fewer wastages. The significant factors that need to be considered in additive manufacturing technology are the mesh resolution, G code arm movements, printing head speed, and metal powders' fusion temperature [30].

In additive manufacturing, fusion deposition modeling, stereolithography liquid additive manufacturing, and metal additive manufacturing are the major classifications used in modern manufacturing industries. In general, the fusion deposition method is used for the materials such as nylon, polylactic acid, and acro nitrile butadiene styrene. In liquid additive manufacturing, liquid resins are used in the manufacturing process. In metal additive manufacturing, the conversion of liquid to the solid phase is not equipped due to the higher melting point of the metal powders. Still, metal powder is heated to reach the fusion temperature. The higher temperature of the platform leads to the fuse of the metal powder layer by layer. Finally, the section of the solid model is built using metal additive manufacturing.

Conventional manufacturing process involves the use of traditional machining techniques such as milling, drilling, and turning to produce parts with a predetermined shape and size. This process follows a subtractive approach, where excess material is removed from a block of material to create the desired shape [31,32]. The process is usually expensive, time consuming, and generates a lot of waste material. On the other hand, additive manufacturing process utilizes various techniques such as 3D printing, laser sintering, and electron beam melting to create parts layer-by-layer [21,22]. This process follows an additive approach, where material is added to create the desired shape. This process is often faster, less expensive, and produces less waste material [23]. Additionally, additive manufacturing allows for the production of complex shapes and geometries that are not possible with conventional manufacturing, allowing for more efficient designs [24,33].

The current state of research on topology optimization for metal additive manufacturing techniques provides the valuable insights for the current study. Nigmatullin *et al.* provided an overview of the use of Fourier analysis to describe multi-periodic signals generated by complex systems [27,34]. Plocher and Panesar's article reviews the current design and structural optimization in additive manufacturing [28], while Rosso *et al.*'s article discusses an optimization workflow in design for additive manufacturing [29]. Ibhadode *et al.*'s article focuses on topology optimization for metal additive manufacturing, including current trends, challenges, and future outlook [30]. Dal Fabbro *et al.*'s article examines the analysis of a preliminary design approach for conformal lattice structures [31], and Helal *et al.*'s article discusses the dimensional structural mass optimization of forged steel connecting rods for aircraft piston engines [32]. The metal additive manufacturing technique uses fine metal powders to build components from the CAD data [35,36]. The G codes generated by the slicer software lead to the movement of the printing head in the X, Y, and Z axes. The platform movement accomplishes the depth of the material. Using metal additive manufacturing techniques, fine metal powders create strong, intricate shapes of 3D printed components. Metal additive manufacturing is used in the aerospace industry to manufacture guide vanes, jet engine nozzles, diffusers, and fuel injectors.

Irrespective of the traditional design constraints, metal additive manufacturing offers the feasibility of manufacturing intricate shapes. The heat sources such as LASER or electron beam are used to heat the metal powder. Metal additive manufacturing works by adding fused metal powder layer by layer. Three methods are majorly used in metal additive manufacturing techniques, *i.e.*, powder bed methods, metal binder heating, and direct energy deposition methods. This article explores the case study of topology optimization of an air compressor piston, and metal additive manufacturing methodology is exhibited.

2 Experimentation: Materials and methods

One horsepower compressor piston is used for reverse engineering to convert the physical component to CAD data. The geometry was created in PTC Creo Elements and exported in Initial Graphics Exchange Specification format. The CAD data is imported into the ANSYS Workbench. The geometry is considered an isotropic material. The geometry has meshed in ANSYS Workbench with the local sizing of 50. Based on the mesh size, the optimization results will vary. The transformation of design optimization from the original model to the optimized model of the compressor piston is illustrated in the figure. The material removal is based on local residual stresses, and the curves are smoothened using geometric tools in the ANSYS Workbench. The experimental trials in ANSYS prove that the smoothness of the curve and the topology-optimized design's accuracy depend on the mesh relevance. The more considerable mesh relevance leads to the poor accuracy of localized stresses. The precise, accurate local stresses in the piston model lead to the metal removal area, which gives the optimized model. It reduces the component's weight and reduces friction and inertia. The friction between the side walls is reduced in this experiment by decreasing the contact surface. The boundary conditions in the ANSYS Workbench are exhibited in the figure, which shows the fixed support, pressure applied in the surface area, and the sliding contacts. The metal additive manufacturing guidelines are illustrated in the literature findings. The selective laser sintering technique is often used for metal powders which relate the powder metallurgy to fuse the metal powders [37,38]. The metal powders' bonding is mainly due to the melting temperature [39,40]. The fusion between the metal powder takes place in four phases: loose powder, initial stage, intermediate stage, and final stage. In the loose powder stage, the density of the powder is high and not sintered. The topology-optimized model is imported in the preform slicer firmware for slicing the standard triangle language (STL) model into layers. The pictorial view of the preform slicer with the topology-optimized piston model is illustrated in Figure 1. The support made for the optimized model is given to the STL model, as exhibited in Figure 2.

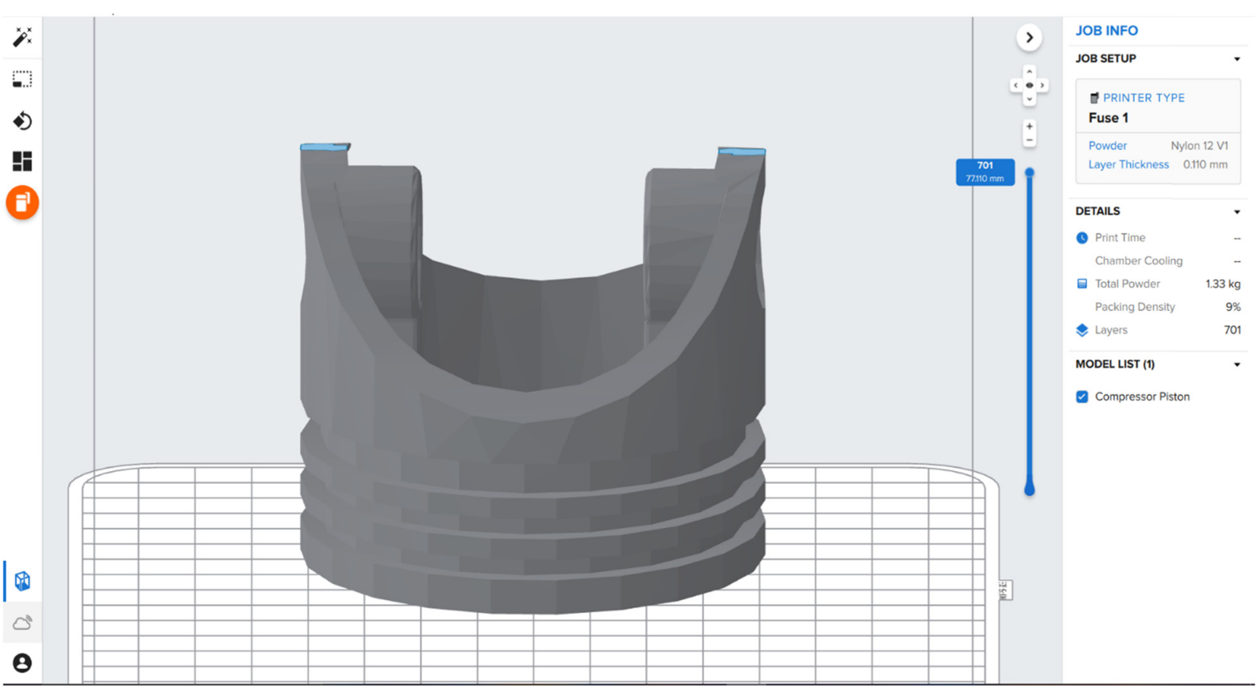

Figure 1: Topology-optimized model in preform metal additive manufacturing slicer formware.

The heating to sinter the metal powder leads to the shrinking of the 3D printed components. After the critical temperature limits of the metal powder in the heating zones, the metal powder fuse with one another [21]. The intermediate zone is also called as fusion zone [22]. The temperature of the 3D printed component is reduced after the intermediate zone. The difference between the selective laser and conventional sintering processes is mainly the pressure applied to the 3D printed materials [41,42]. In the conventional sintering process, the metal powders are placed in the die, and the pressure is involved with the binding agents. Whereas in metal additive manufacturing, a 3D printing head is used to project the LASER source in the metal powder layer.

The fusion takes place layer by layer after the fusion of the previous layers. The cross-section of the component is printed after the consequent layers using STL files. The standard triangulation language is used in the slicer software, and the respective G codes are generated to trace the cross-section/layers of the component. Several types of research have been carried out on the material strength of the metal 3D printed parts. The mechanical properties of the metal 3D published features are based on the preheating and heating temperature [23]. The fusion of metal powders leads to bonding between the powder particulates. The powder metallurgy technique is used in selective laser sintering 3D printing since the intricate shapes can be manufactured easily in 3D printing techniques with less manufacturing cost. The literature on the topology optimization is studied and reverse engineering of the air compressor piston is done using a 3D scanner application [43,44].

The transition of existing model piston to topology-optimized air compressor piston is illustrated in Figure 3 and the methodology is illustrated in Figure 4.

The CAD model is prepared by importing the files into the CAD environment using Creo Elements, and the dimensions are validated with the physical object (air compressor piston). CAD model of the piston is depicted in Figure 5. This research selects a reciprocating compressor range of 2,000 bar, and topology optimization is done in the ANSYS Workbench, the process flow is illustrated in Figure 6. The optimization technique and metal additive manufacturing guidelines are explained in Section 3.

3 Results and discussion

The experimental values for each mesh relevance in ANSYS finite element model is observed and validated with the real time compressor piston. In ANSYS work bench, the mesh relevance is varied from 0 to 10 and the optimum stress values are obtained in mesh relevance of 3. The smoothness of the curve for topology optimization with precise and accurate results are achieved in this mesh relevance.

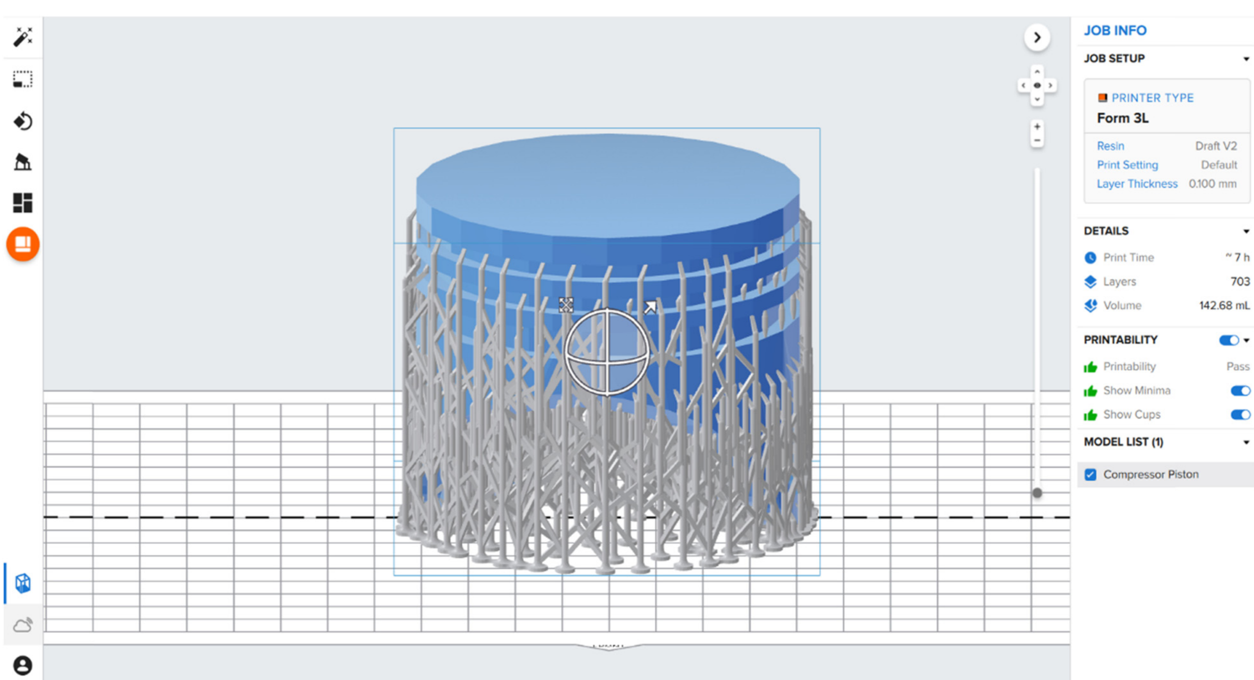

Figure 2: Metal additive manufacturing of topology-optimized piston model.

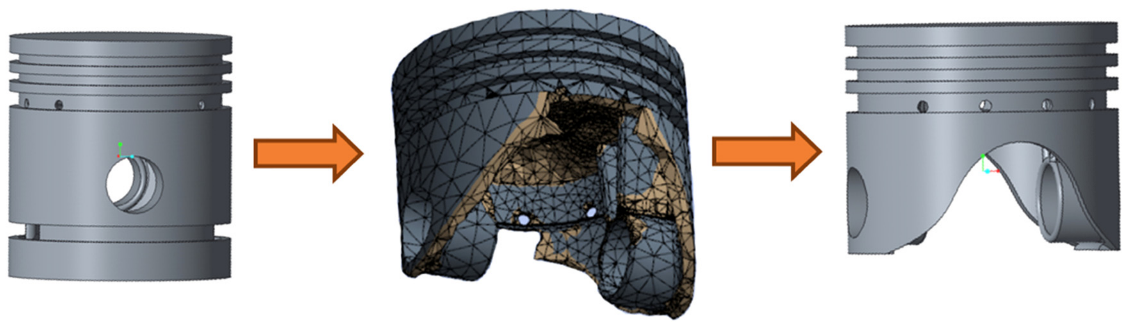

Figure 3: Transition of existing model piston to topology-optimized air compressor piston.

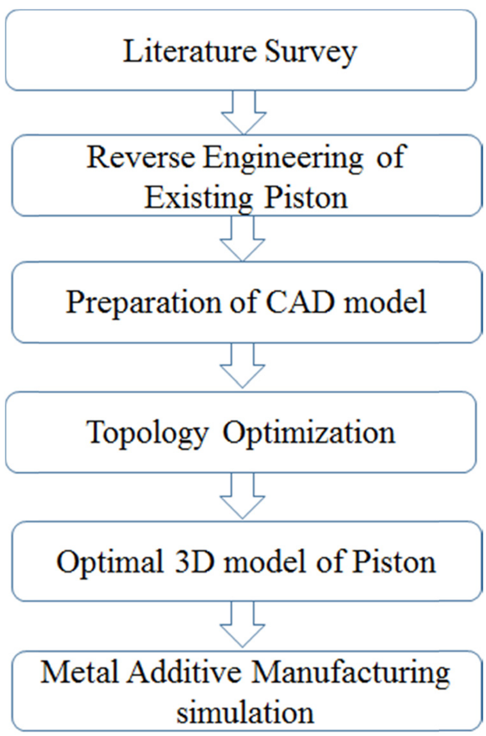

Figure 4: Methodology adopted in topology optimization and metal additive manufacturing.

The free mesh is selected for all the sides and the local stress is calculated for metal removal operation. The reduction in inertia of the piston is due to the reduction in mass which leads to less power consumption in operation [24]. The mass of the compressor piston is compared with the topology-optimized and conventional piston model [45–47]. In the conventional model, 258 g of piston is weighed using digital balance and in Creo Elements, mass properties are obtained at a weight of 255 g. The local stresses are determined and the material is removed in ANSYS work bench which leads to the weight of 174 g. In topology-optimized model, 81 g of weight is reduced which leads to reduction in power consumption. The mass comparison of the conventional air compressor piston and the topology optimized piston is illustrated in Figure 7.

The inertial load of the piston acts on the drive of the compressor such as motor or engine. The drive consumes power according to the inertial load, the inertial load is calculated for the topology-optimized piston and conventional compressor piston and the same is illustrated in Figure 8 [48–50]. In the conventional air compressor piston, the inertial load of 2.5 N is achieved to drive it. The load acting on the drive which consumes power to overcome the gravitational force and frictional forces are taken into account [51–53]. The inertial load is reduced to 1.75 N in topology-optimized piston. The inertial load of 0.74 N is reduced.

The torque required in the crank shaft to achieve the reciprocating motion in the compressor assembly is calculated for the conventional piston model and topology-optimized model. The diagrammatic representation is shown in Figure 9 for the torque comparison. The torque of 0.375 Nm is required in conventional piston model and 0.361 Nm of torque is required in topology-optimized piston model. The comparative study of torque reduction, inertial load reduction, and mass reduction is done using the bore length ratio, swept volume of the cylinder, and assuming the air velocity of 500 m/s in to the compressor cylinder. The assumptions made in the calculations and deriving the mass, torque, and inertial load are exhibited in the calculations section [54–56].

Torque calculations:

Piston diameter = 70 mm.

Assumptions:

Average velocity of air = 500 m/s,

and bore/stroke ratio, square stroke is considered.

So, $L = D$, $L = 70$ mm.

Clearance volume of the cylinder is 10% of swept volume.

Power = 2 hp,

Speed, $N = 1{,}440$ rpm,

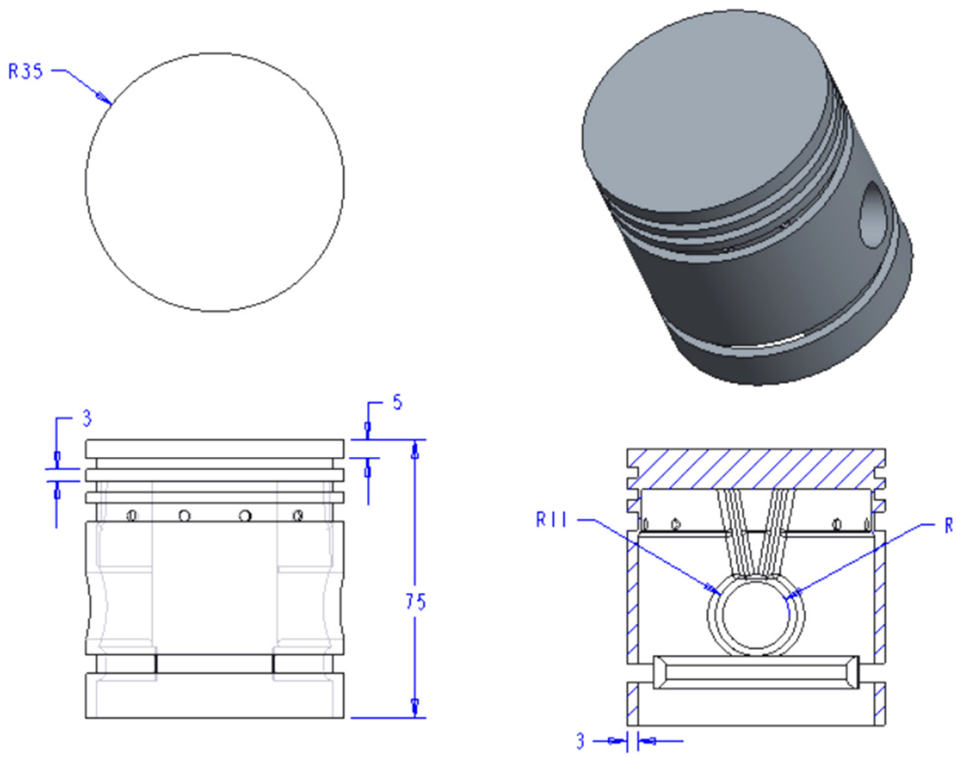

Figure 5: The conventional air compressor CAD model from reverse engineering.

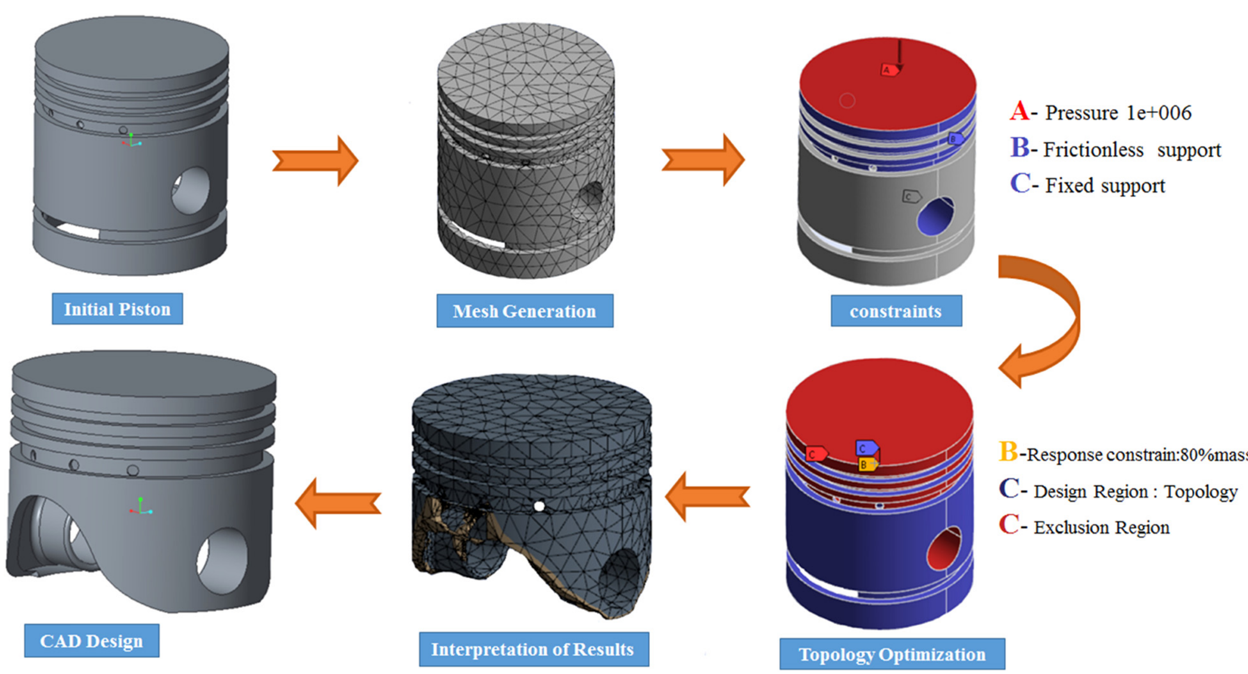

Figure 6: Transition of conventional air compressor piston to topology-optimized piston in ANSYS work bench environment.

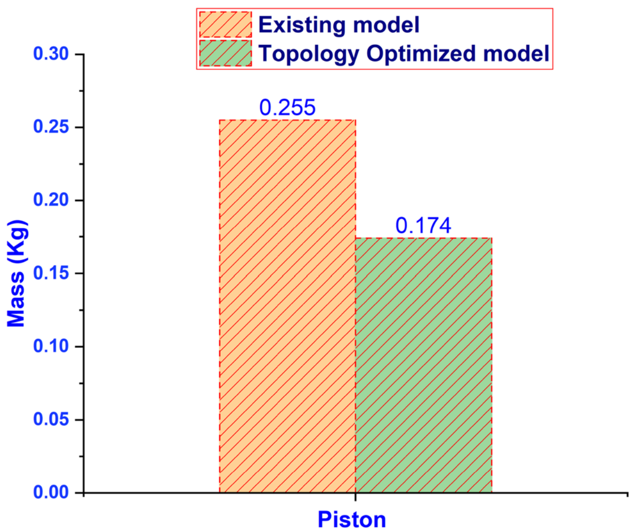

Figure 7: The mass comparison of conventional air compressor piston and topology-optimized piston.

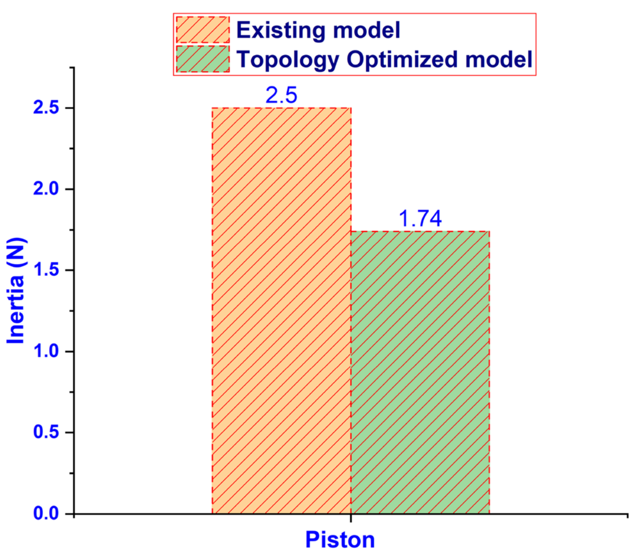

Figure 8: Inertia load comparison between conventional air compressor piston and topology-optimized piston.

Torque (Nm) = 9.5488 × Power (kW)/Speed (rpm),

Torque = 16.37 Nm.

Cross-sectional area of cylinder = $\pi r^2 = \pi(35)^2 = 3848.45 \ \ \mathrm{mm}^2$

Cross-sectional area of cylinder = 3.84 m^2,

and flow rate, Q = Area of cylinder × Velocity of air

= 3.84 × 500

Q = 1,920 m^3/s

Swept volume, Vs = $L \times (\pi(35)^2)$

= $75 \times (\pi(35)^2)$

= $288,633.75 \ \ \mathrm{mm}^3$

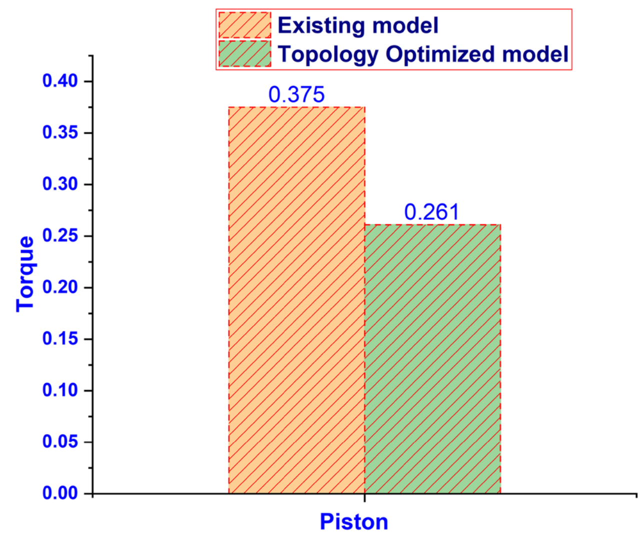

Figure 9: Torque comparison between conventional air compressor piston and topology-optimized piston.

Vs = 288.6 m^3

Assuming clearance volume of the cylinder is **10%** of swept volume,

clearance volume, Vc = 28.8m^3.

Total volume of the cylinder = Swept volume + clearance volume

= 288.6 + 28.8.

Thus, total volume of the cylinder = 317.4 m^3.

Compression ratio, $r = \frac{\mathrm{Vs} + \mathrm{Vc}}{\mathrm{Vc}}$

$= \frac{288.6 + 28.8}{28.8} r = 11.00.$

Mass properties for conventional air compressor piston model:

Mass = 0.255 kg,

Inertia = Mass × Acceleration

= 0.255 × 9.81

Inertia = 2.5 N.

Torque, τ = radius of crankshaft × force (inertia)

= 0.15 × 2.5

τ = 0.375 Nm

Power = Torque (Nm) × Speed (rpm)/9.5488

= 0.375 × 1,440/9.5488

= 56.55 W

Power = 0.056 kW.

Mass properties for topology-optimized piston model:

Mass = 0.178 kg,

Inertia = Mass × Acceleration

= 0.178 × 9.81

Mass = 0.178 kg.

Inertia = Mass × Acceleration

= 0.178 × 9.81

Inertia = 1.74 N.

Torque, τ = radius of crankshaft × force (inertia)

= **0.15** × **1.74**

τ = 0.261 Nm

Power = Torque (Nm) × Speed (rpm)/9.5488

= 0.261 × 1,440/9.5488

= 39.35 W

Power = **0.039 kW.**

The power required to operate the compressor piston is calculated in the real-time environment for the conventional piston model and compared with the numerical solutions [57–59]. The numerical technique yields the power of 0.056 kW required to drive the air compressor to reach the pressure of 50 PSI as exhibited in Figure 10. The comparison was made between the conventional and topology-optimized piston models in the same testing conditions of maximum pressure of 50 PSI. The pressure developed in the topology-optimized model is compared in a real-time environment and is increased with less power consumption to drive the compressor unit [25,26].

4 Comparative analysis of the findings utilizing two distinct processes

A comparison study between a traditional manufacturing process and an additive manufacturing process for the production of an air compressor piston is portrayed in this section. The two different types of piston models' required masses, inertia loads, and torques, which are compared in the study. The mesh relevance of three was discovered to be optimal when the finite element model was used in ANSYS Workbench to optimize the topology of the additive manufacturing process [60–62]. In this mesh relevance, the curve was achieved with accuracy and smoothness. The local stress for the metal removal operation was calculated, and since the mass of the piston was decreased, its inertia was also decreased, resulting in a reduction in operating power consumption [27].

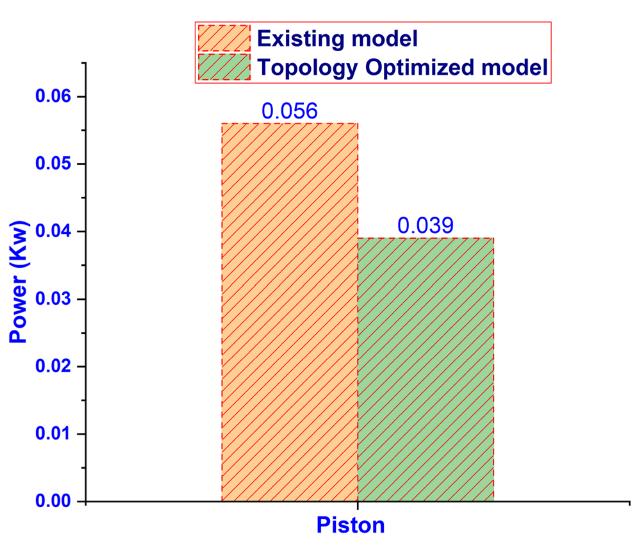

Figure 10: Power comparison between conventional air compressor piston and topology-optimized piston.

By weighing them with a digital balance and obtaining the mass properties with CREO Elements, the mass of the topology-optimized piston model and the conventional air compressor piston model were compared. The weight of the conventional model was 174 g, while the topology-optimized model weighed only 81 g thanks to the determination of the local stresses and the removal of material in ANSYS Workbench. Both models' inertial loads for the piston were calculated, and Figure 8 shows the results. The topology-optimized model's inertial load was found to be 1.75 N, a reduction of 0.74 N from the conventional model's inertial load of 2.5 N.

Additionally, the two models' respective torque requirements for the reciprocating motion in the compressor assembly were contrasted. The topology-optimized piston model required 0.361 Nm of torque compared to the conventional piston model's 0.375 Nm. Utilizing the bore length ratio, the swept volume of the cylinder, and the assumption that air would enter the compressor cylinder at a speed of 500 m/s, a comparative study of torque reduction, inertial load reduction, and mass reduction was conducted [63–65]. The calculations section lists the underlying presumptions used to derive the mass, torque, and inertial load [28,66,67].

The real-time compressor piston was used to observe and validate the experimental values for each mesh relevance in the ANSYS finite element model. The ideal stress values were obtained in ANSYS Workbench at a mesh relevance of 3, which was varied from 0 to 10. In this mesh relevance, the curve's smoothness was achieved through topology optimization, producing accurate and precise results. The topology-optimized and conventional piston models' masses of the compressor piston were compared [68,69]. The weight in the conventional model was greater than that in the topology-optimized model, which increased power consumption [29,70,71]. The compressor piston's mass was decreased owing to topology optimization and metal additive manufacturing techniques, which also resulted in a decrease in power consumption [30,68,72].

For the purpose of producing an air compressor piston, the study compared additive manufacturing with traditional manufacturing methods. Comparing the topology-optimized piston model to the conventional model, it was found to have less mass, inertial load, and torque. Finite element modeling and ANSYS Workbench were used to obtain the results. The study demonstrates the potential advantages of using additive manufacturing to lower power consumption and enhance air compressor piston performance [31,32].

5 Conclusion

The findings from the finite element analysis illustrate that increasing mesh relevance leads to a decrease in the precision and accuracy of the topology optimization curves. The local stress regions will be accurate with the optimized mesh relevance. The results observed in the conventional air compressor piston model and topology-optimized piston model is that 2.04% of mass is reduced in the topology-optimized air compressor model. The power required to drive the air compressor in the topology-optimized model is reduced to 0.1%, which reduces the power consumption of electricity and conventional fossil fuels.

Acknowledgments: The authors extend their appreciation to the Deanship of Scientific Research at King Khalid University (KKU) for funding this research through the Research Group Program Under the Grant Number: (R.G.P.1/349/43).

Funding information: This research was funded by the Deanship of Scientific Research at King Khalid University (KKU) through the Research Group Program Under the Grant Number: (R.G.P.1/349/43).

Author contributions: Conceptualization: G.S., S.Y., S.K.R., D.K.S., G.G., and S.S.; methodology: G.S., S.Y., S.K.R., D.K.S., G.G., and S.S.; formal analysis: G.S., S.Y., S.K.R., D.K.S., G.G., S.S., and A.K.; investigation: G.S., S.Y., S.K.R., D.K.S., G.G., and S.S.; writing – original draft preparation: G.S., S.Y., S.K.R., D.K.S., G.G., and S.S.; writing – review and editing: S.S., A.K., C.L., and M.A.; supervision: S.S., A.K., C.L., and M.A.; project administration: S.S. and M.A.; funding acquisition: S.S. and M.A. All authors have accepted responsibility for the entire content of this manuscript and approved its submission.

Conflict of interest: The authors state no conflict of interest.

References

[1] Tempiam A, Kachapongkun P, Rattanadecho P, Prommas R. Experimental investigation of vortex tube for reduction air inlet of a reciprocating air compressor. Case Stud Therm Eng. 2020;19:100617.
[2] Meli E, Rindi A, Ridolfi A, Furferi R, Buonamici F, Iurisci G, et al. Design and production of innovative turbomachinery components via topology optimization and additive manufacturing. Int J Rotating Mach. 2019;2019:1–12.
[3] Andrearczyk A, Bagiński P, Klonowicz P. Numerical and experimental investigations of a turbocharger with a compressor wheel made of additively manufactured plastic. Int J Mech Sci. 2020;178:105613.
[4] Blakey-Milner B, Gradl P, Snedden G, Brooks M, Pitot J, Lopez E, et al. Metal additive manufacturing in aerospace: A review. Mater Des. 2021;209:1–13.
[5] Fayaz G, Kazemzadeh S. Towards additive manufacturing of compressor impellers: 3D modeling of multilayer laser solid freeform fabrication of nickel alloy 625 powder mixed with nano-CeO_2 on AISI 4140. Addit Manuf. 2018;20:182–8.
[6] Guo W, Zuo Z, Sun J, Hou H, Liang Q, Chen H. Experimental investigation on off-design performance and adjustment strategies of the centrifugal compressor in compressed air energy storage system. J Energy Storage. 2021;38:102515.
[7] Kim EH, Choi HH, Jung YG. Fabrication of a ceramic core for an impeller blade using a 3D printing technique and inorganic binder. J Manuf Process. 2020;53:43–7.
[8] Kulikov AA, Sidorova AV, Balanovskiy AE. Process design for the wire arc additive manufacturing of a compressor impeller. IOP Conf Ser: Mater Sci Eng. 2020 Nov;969(1):012098. IOP Publishing.
[9] Li J, Liu Y, Du J, Zhang H, Nie C. Implementation of stability-enhancement with tip air injection in a multi-stage axial flow compressor. Aerosp Sci Technol. 2021;113:106646.
[10] Dejun JIA, Fanchun LI, Zhang Y. 3D-printing process design of lattice compressor impeller based on residual stress and deformation. Sci Rep. 2020;10(1):1–11.
[11] Zhang Y, Li F, Jia D. Lightweight design and static analysis of lattice compressor impeller. Sci Rep. 2020;10(1):1–10.
[12] Gao X, Liu Y. Design, modeling and characteristics research of a novel self-air-cooling reciprocating compressor. Int J Refrig. 2021;128:62–70.
[13] Wiratkasem K, Pattana S, Tippayawong KY, Tippayawong N. Developing the high energy performance standards for oil-injected air-cooled screw air compressor for Thailand. Energy Rep. 2020;6:617–21.
[14] Ford S, Despeisse M. Additive manufacturing and sustainability: an exploratory study of the advantages and challenges. J Clean Prod. 2016;137:1573–87.
[15] Aw KT, Ooi KT. A review on sliding vane and rolling piston compressors. Machines. 2021;9(6):125.
[16] Gouda EM, Fan Y, Benaouicha M, Neu T, Luo L. Review on liquid piston technology for compressed air energy storage. J Energy Storage. 2021;43:103111.
[17] Hu Y. Recent progress in field-assisted additive manufacturing: Materials, methodologies, and applications. Mater Horiz. 2021;8(3):885–911.
[18] Pochari C. Process Intensified Ammonia Plants based on Advanced Compressor Technology for Distributed Production. SSRN 3884636. 2021.

[19] Venkatesh S, Sivapirakasam SP, Sakthivel M, Ganeshkumar S, Prabhu MM, Naveenkumar M. Experimental and numerical investigation in the series arrangement square cyclone separator. Powder Technol. 2021;383:93–103.
[20] Ganeshkumar S, Thirunavukkarasu V, Sureshkumar R, Venkatesh S, Ramakrishnan T. Investigation of wear behaviour of silicon carbide tool inserts and titanium nitride coated tool inserts in machining of EN8 steel. Int J Mech Eng Technol. 2019;10(01):1862–73.
[21] Kumar SG, Thirunavukkarasu V. Investigation of tool wear and optimization of process parameters in turning of EN8 and EN36 steels. Asian J Res Soc Sci Humanit. 2016;6(11):237–43.
[22] Ganeshkumar S, Sureshkumar R, Sureshbabu Y, Balasubramani S. A review on cutting tool measurement in turning tools by cloud computing systems in industry 4.0 and IoT. GIS Sci J. 2020;7(8):1–7.
[23] Ganeshkumar S, Sureshkumar R, Sureshbabu Y, Balasubramani S. A numerical approach to cutting tool stress in CNC turning of EN8 steel with silicon carbide tool insert. Int J Sci Technol Res. 2019;8(12):3227–31.
[24] Gokilakrishnan G, Ganeshkumar S, Anandakumar H, Vigneshkumar M. A critical review of production distribution planning models. In: 2021 7th International Conference on Advanced Computing and Communication Systems (ICACCS). IEEE: Vol. 1, 2021 Mar. p. 2047–51.
[25] Ganeshkumar S, Venkatesh S. Manufacturing techniques and applications of multifunctional metal matrix composites. Funct Compos Mater Manuf Technol Exp Appl. 2022;16(10):105173.
[26] Ganeshkumar S, Kumar SD, Magarajan U, Rajkumar S, Arulmurugan B, Sharma S, et al. Investigation of tensile properties of different infill pattern structures of 3D-printed PLA polymers: Analysis and validation using finite element analysis in ANSYS. Materials. 2022;15(15):5142.
[27] Nigmatullin RR, Alexandrov VS, Agarwal P, Jain S, Ozdemir N. Description of multi-periodic signals generated by complex systems: NOCFASS - New possibilities of the Fourier analysis. Numer Algebra Control Optim. 2022;1:1–19. doi: 10.3934/naco.2022008.
[28] Plocher J, Panesar A. Review on design and structural optimisation in additive manufacturing: Towards next-generation lightweight structures. Mater Des. 2019;183:108164.
[29] Rosso S, Uriati F, Grigolato L, Meneghello R, Concheri G, Savio G. An optimization workflow in design for additive manufacturing. Appl Sci. 2021;11(6):2572.
[30] Ibhadode O, Zhang Z, Sixt J, Nsiempba KM, Orakwe J, Martinez-Marchese A, et al. Topology optimization for metal additive manufacturing: Current trends, challenges, and future outlook. Virtual Phys Prototyp. 2023;18(1):e2181192.
[31] Dal Fabbro P, Rosso S, Ceruti A, Boscolo Bozza D, Meneghello R, Concheri G, et al. Analysis of a Preliminary Design Approach for Conformal Lattice Structures. Appl Sci. 2021;11(23):11449.
[32] Helal M, Felemban BF, Alharthi A, Almalki S, Fathallah E, Elsherbiny AA, et al. Dimensional structural mass optimization of forged steel connecting rod for aircraft piston engine. IOP Conf Ser: Mater Sci Eng. 2021 Aug;1172(1):012001 IOP Publishing.
[33] Song F, Liu Y, Shen D, Li L, Tan J. Learning control for motion coordination in wafer scanners: Toward gain adaptation. IEEE Trans Ind Electron. 2022;69(12):13428–38. doi: 10.1109/TIE.2022.3142428.
[34] Song F, Liu Y, Jin W, Tan J, He W. Data-driven feedforward learning with force ripple compensation for wafer stages: A variable-gain robust approach. IEEE Trans Neural Netw Learn Syst. 2022;33(4):1594–608. doi: 10.1109/TNNLS.2020.3042975.
[35] Chen J, Wang Q, Cheng HH, Peng W, Xu W. A review of vision-based traffic semantic understanding in ITSs. IEEE Trans Intell Transp Syst. 2022;23(11):19954–79. doi: 10.1109/TITS.2022.3182410.
[36] Bai X, Huang M, Xu M, Liu J. Reconfiguration optimization of relative motion between elliptical orbits using Lyapunov-Floquet transformation. IEEE Trans Aerosp Electron Syst. 2023;59(2):923–36. doi: 10.1109/TAES.2022.3193089.
[37] Sun W, Liu Y, Li M, Cheng Q, Zhao L. Study on heat flow transfer characteristics and main influencing factors of waxy crude oil tank during storage heating process under dynamic thermal conditions. Energy. 2023;269:127001. doi: 10.1016/j.energy.2023.127001.
[38] Sun T, Peng L, Ji X, Li X, Rodellar J. A Half-Cycle Negative-Stiffness Damping Model and Device Development. Struct Control Health Monit. 2023;2023:4680105. doi: 10.1155/2023/4680105.
[39] Tian L, Jin B, Li L. Axial Compressive Mechanical Behaviors of a Double-Layer Member. J Struct Eng. 2023;149(8):4023110. doi: 10.1061/JSENDH.STENG-12175.
[40] Yu J, Shi Z, Dong X, Li Q, Lv J, Ren Z. Impact time consensus cooperative guidance against the maneuvering target: Theory and experiment. IEEE Trans Aerosp Electron Syst. 2023;59(4):4590–603. doi: 10.1109/TAES.2023.3243154.
[41] Li D, Ge SS, Lee TH. Fixed-time-synchronized consensus control of multiagent systems. IEEE Trans Control Netw Syst. 2021;8(1):89–98. doi: 10.1109/TCNS.2020.3034523.
[42] Zhou S, Zhou G, Liu X, Zhao H. Dynamic Freewheeling Control for SIDO Buck Converter With Fast Transient Performance, Minimized Cross-Regulation, and High Efficiency. IEEE Trans Ind Electron. 2023;70(2):1467–77. doi: 10.1109/TIE.2022.3156169.
[43] Zhou S, Zhou G, He M, Mao S, Zhao H, Liu G. Stability Effect of Different Modulation Parameters in Voltage-Mode PWM Control for CCM Switching DC-DC Converter. IEEE Trans Transp Electrif. 2023;1:1–15. doi: 10.1109/TTE.2023.3293811.
[44] Bai X, He Y, Xu M. Low-thrust reconfiguration strategy and optimization for formation flying using Jordan normal form. IEEE Trans Aerosp Electron Syst. 2021;57(5):3279–95. doi: 10.1109/TAES.2021.3074204.
[45] Hu W, Wang T, Chu F. A novel Ramanujan digital twin for motor periodic fault monitoring and detection. IEEE Trans Ind Inform. 2023;1:1–9. doi: 10.1109/TII.2023.3248110.
[46] Yu H, Zhang J, Fang M, Ma T, Wang B, Zhang Z, et al. Bio-inspired strip-shaped composite composed of glass fabric and waste selvedge from A. *pernyi* silk for lightweight and high-impact applications. Compos Part A: Appl Sci Manuf. 2023;174:107715. doi: 10.1016/j.compositesa.2023.107715.
[47] Li H, Si S, Yang K, Mao Z, Sun Y, Cao X, et al. Hexafluoroisopropanol based silk fibroin coatings on AZ31 biometals with enhanced adhesion, corrosion resistance and biocompatibility. Prog Org Coat. 2023;184:107881. doi: 10.1016/j.porgcoat.2023.107881.
[48] Yang K, Guan J, Numata K, Wu C, Wu S, Shao Z, et al. Integrating tough Antheraea pernyi silk and strong carbon fibres for impact-critical structural composites. Nat Commun. 2019;10(1):3786. doi: 10.1038/s41467-019-11520-2.
[49] Sun W, Wang H, Qu R. A novel data generation and quantitative characterization method of motor static eccentricity with adversarial network. IEEE Trans Power Electron. 2023;38(7):8027–32. doi: 10.1109/TPEL.2023.3267883.
[50] Lu H, Zhu Y, Yin M, Yin G, Xie L. Multimodal fusion convolutional neural network with cross-attention mechanism for internal defect detection of magnetic tile. IEEE Access. 2022;10:60876–86. doi: 10.1109/ACCESS.2022.3180725.

[51] Huang S, Huang M, Lyu Y. Seismic performance analysis of a wind turbine with a monopile foundation affected by sea ice based on a simple numerical method. Eng Appl Comput Fluid Mech. 2021;15(1):1113–33. doi: 10.1080/19942060.2021.1939790.

[52] Shen D, Cheng M, Wu K, Sheng Z, Wang J. Effects of supersonic nozzle guide vanes on the performance and flow structures of a rotating detonation combustor. Acta Astronaut. 2022;193:90–9. doi: 10.1016/j.actaastro.2022.01.002.

[53] Liu F, Sun Z, Bian H, Ding M, Meng X. Identification and classification of the flow pattern of hydrogen-air-steam mixture gas under steam condensation. Int J Therm Sci. 2023;183:107854. doi: 10.1016/j.ijthermalsci.2022.107854.

[54] Li H, Li G, Li L. Comparative investigation on combustion characteristics of ADN-based liquid propellants in inert gas and oxidizing gas atmospheres with resistive ignition method. Fuel. 2023;334:126742. doi: 10.1016/j.fuel.2022.126742.

[55] Rong G, Cheng M, Sheng Z, Liu X, Zhang Y, Wang J. Investigation of counter-rotating shock wave and wave direction control of hollow rotating detonation engine with Laval nozzle. Phys Fluids. 2022;34(5):56104. doi: 10.1063/5.0089207.

[56] Wang J, Liang F, Zhou H, Yang M, Wang Q. Analysis of position, pose and force decoupling characteristics of a 4-UPS/1-RPS parallel grinding robot. Symmetry. 2022;14(4):825. doi: 10.3390/sym14040825.

[57] Liao D, Zhu S, Keshtegar B, Qian G, Wang Q. Probabilistic framework for fatigue life assessment of notched components under size effects. Int J Mech Sci. 2020;181:105685. doi: 10.1016/j.ijmecsci.2020.105685.

[58] Niu X, Zhu S, He J, Liao D, Correia JAFO, Berto F, et al. Defect tolerant fatigue assessment of AM materials: Size effect and probabilistic prospects. Int J Fatigue. 2022;160:106884. doi: 10.1016/j.ijfatigue.2022.106884.

[59] Wu H, Zhang Z, Zhang F, Roberts WL. Time-resolved low-pressure air-assisted spray performance and unsteadiness evaluation. Phys Fluids. 2023;35(4):43335. doi: 10.1063/5.0145761.

[60] Xia C, Zhu Y, Zhou S, Peng H, Feng Y, Zhou W, et al. Simulation study on transient performance of a marine engine matched with high-pressure SCR system. Int J Engine Res. 2022;24(4):1327–45. doi: 10.1177/14680874221084052.

[61] Liu L, Peng Y, Zhang W, Ma X. Concept of rapid and controllable combustion for high power-density diesel engines. Energy Convers Manag. 2023;276:116529. doi: 10.1016/j.enconman.2022.116529.

[62] Wang Y, Zhou X, Liu L. Feasibility study of hydrogen jet flame ignition of ammonia fuel in marine low speed engine. Int J Hydrog Energy. 2022;48(1):327–36. doi: 10.1016/j.ijhydene.2022.09.198.

[63] Liu L, Mei Q, Jia W. A flexible diesel spray model for advanced injection strategy. Fuel. 2022;314:122784. doi: 10.1016/j.fuel.2021.122784.

[64] Yang M, Kong M, Li C, Long Y, Zhang Y, Sharma S, et al. Temperature field model in surface grinding: A comparative assessment. Int J Extreme Manuf. 2023. in press doi: 10.1088/2631-7990/acf4d4.

[65] Jia D, Li C, Liu J, Zhang Y, Yang M, Gao T, et al. Prediction model of volume average diameter and analysis of atomization characteristics in electrostatic atomization minimum quantity lubrication. Friction. 2023;11:2107–31. doi: 10.1007/s40544-022-0734-2.

[66] Liu M, Li C, Zhang Y, Yang M, Gao T, Cui X, et al. Analysis of grain tribology and improved grinding temperature model based on discrete heat source. Tribol Int. 2023;180:108196. doi: 10.1016/j.triboint.2022.108196.

[67] Duan Z, Li C, Zhang Y, Yang M, Gao T, Liu X, et al. Mechanical behavior and Semiempirical force model of aerospace aluminum alloy Milling using Nano biological lubricant. Front Mech Eng. 2022;48(1):327–36. doi: 10.1007/s11465-022-0720-4.

[68] Wang Y, Mushtaq RT, Ahmed A, Ahmed A, Rehman M, Rehman M, et al. Additive manufacturing is sustainable technology: Citespace based bibliometric investigations of fused deposition modeling approach. Rapid Prototyp J. 2021;28(4):654–75. doi: 10.1108/RPJ-05-2021-0112.

[69] Chohan JS, Kumar R, Singh TB, Singh S, Sharma S, Singh J, et al. Taguchi S/N and TOPSIS based optimization of fused deposition modelling and vapor finishing process for manufacturing of ABS plastic parts. Materials (MDPI). 2020;13(22):5176. doi: 10.3390/ma13225176.

[70] Banerjee N, Sen A, Ghosh PS, Biswas AR, Sharma S, Kumar A, et al. Prediction and simulation of mechanical properties of borophene reinforced epoxy nanocomposites using molecular dynamics and FEA analysis. Rev Adv Mater Sci. 2023;62(1):20220322. doi: 10.1515/rams-2022-0322.

[71] Saxena A, Dwivedi SP, Kaushik A, Sharma S. Investigation on mechanical properties of ZTA + Cr_3C_2 + Ni reinforced EN31 steel-based composite material: Micromechanical FEA. Part E: J Process Mech Eng. 2022;237(4):1378–93. doi: 10.1177/09544089221113141.

[72] Mushtaq RT, Wang Y, Khan AM, Rehman M, Li X, Sharma S. A post-processing laser polishing method to improve process performance of 3D printed new Industrial Nylon-6 polymer. J Manuf Process. 2023 Sept;101:546–60. doi: 10.1016/j.jmapro.2023.06.019.